IOP Conf. Series: Materials Science and Engineering **278** (2017) 012140 doi:10.1088/1757-899X/278/1/012140

Influence of minor geometric features on Stirling pulse tube cryocooler performance

T Fang[1], P S Spoor[2], S M Ghiaasiaan[1] and M Perrella[1]

[1]Georgia Tech Cryo Lab, G.W. Woodruff School of Mechanical Engineering, Georgia Institute of Technology, Atlanta, GA 30332 USA

[2]Chart, Biomedical Division, Chart Inc., Troy, New York 12188

Email: mghiaasiaan@gatech.edu

Abstract. Minor geometric features and imperfections are commonly introduced into the basic design of multi-component systems to simplify or reduce the manufacturing expense. In this work, the cooling performance of a Stirling type cryocooler was tested in different driving powers, cold-end temperatures and inclination angles. A series of Computational Fluid Dynamics (CFD) simulations based on a prototypical cold tip was carried out. Detailed CFD model predictions were compared with the experiment and were used to investigate the impact of such apparently minor geometric imperfections on the performance of Stirling type pulse tube cryocoolers. Predictions of cooling performance and gravity orientation sensitivity were compared with experimental results obtained with the cryocooler prototypes. The results indicate that minor geometry features in the cold tip assembly can have considerable negative effects on the gravity orientation sensitivity of a pulse tube cryocooler.

1. Introduction

Stirling-type pulse tube cryocoolers (PTCs) with inertance tube were first introduced in 1990s [1, 2]. High reliability and mechanical simplicity make PTCs attractive to some applications. The cold-tip assembly, especially the pulse tube, is a critical component that can directly affect the cooling performance of PTCs. Several loss mechanisms in pulse tubes have been studied including Rayleigh streaming [3], Gedeon streaming [4], shuttle heat transport [5] and convective losses.

Convective losses are usually more significant. Unfavorable gravity orientation and geometry imperfections like diameter mismatches in the conjunction between components can cause notable convective losses. Thummes et al. [6] indicated that, in many PTCs, unfavorable gravity orientation can result in significant loss in cooling power because of the buoyancy effects. Swift and Backhaus [7, 8] experimentally analyzed the phenomenon and developed an analogous theory to explain the convective loss caused by gravity. In their theory, a non-dimensional pulse tube convection number, N_{ptc}, was used as an indicator of gravitational sensitivity. N_{ptc} can be calculated using oscillation frequency, flow displacement and pulse tube aspect ratio. Mulcahey [9] developed system-level and component-level computational fluid dynamic (CFD) approaches to investigate the phenomenon. Fang et al. [10] collected and compared the results of experiments and CFD simulations. Their work indicated that, in comparison with CFD models having similar N_{ptc}, experiments were generally more sensitive to misalignment with respect to gravity orientation. The reason could be some minor geometric features that exist in PTC

prototypes which are not fully resolved by CFD models. Conrad et al. [11] studied the effect of geometric diameter change between different components using CFD simulations. Their work suggested that the sharp-edged transitions between components of different diameters can increase the non-uniformity of flow which may reduce cooling power. Tapered transition yielded better cooling performance. Among the geometry imperfections, the conjuctions between pulse tube and flow striaghtener chambers have the most pronounced effect on cooling power.

In Swift and Backhaus's theory [7, 8], the problem of gravity sensitivity is analogized to an inverted pendulum. However, if other streaming effects are strong, such as the streaming caused by diameter change between components [11], the velocity profile will not be uniform and the analogy is less applicable. As shown in [10], the experimental data were scattered while CFD simulations of Fang et al. showed a rather monotonic and smooth trend. It is possible that the experiments have minor geometric features and imperfections that were not fully resolved by CFD models.

In this study, a PTC prototype was experimentally tested to yield its cooling performance at two different driving powers, two different cold-end temperatures and five different gravity orientations. A two-dimensional CFD model was developed and validated using the experimental data, and was then utilized to investigate the effects of minor geometry features or imperfections that may exist in conjunction between the pulse tube and the flow straightener of the PTC. Due to the restrictions of 2D modeling, the CFD focused on two gravity orientations, vertical with cold head down (0°) (i.e., the ideal condition), and vertical with cold head up (180°). A parametric study regarding the size of the diameter change, the shape of the edge (sharp or round) and the size of the gap between flow straightener and the edge was carried out using the CFD model.

2. Experimental Setup

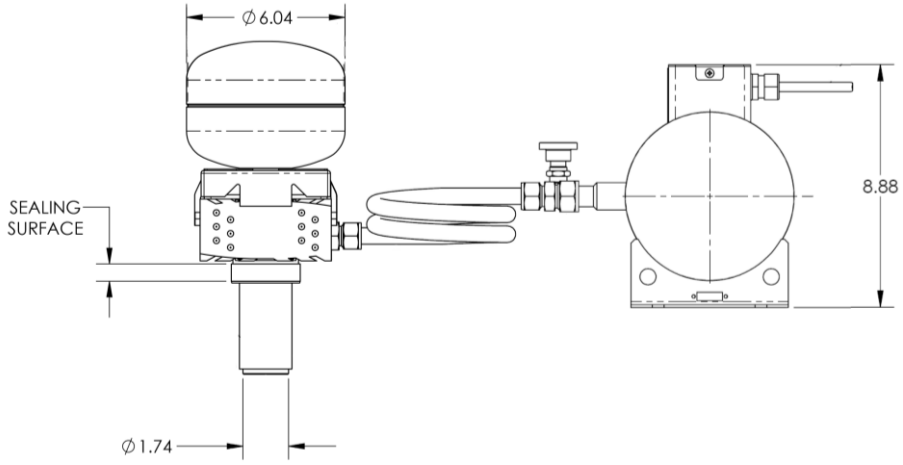

Figure 1. Dimensions of the PTC prototype.

In this work, a commercial PTC prototype provided by Chart Industries, Inc., was tested experimentally. Some dimensions of the PTC prototype are shown in figure 1. The PTC has a coaxial cold tip and is driven by a 60 Hz wave generator. Figure 2 shows the PTC and the vacuum chamber on which it was mounted. The vacuum chamber can be rotated from vertical position (0°, expecting no cooling deterioration caused by gravity) all the way to upside down (180°). The cold tip was sealed inside the vacuum chamber and covered by a radiation shield. A machined copper test plate, as shown in figure 3, was attached to the cold-end of the cold tip. Two 25 W heaters were installed in the through holes of the test plate to provide the cooling load for the PTC. A LakeShore DT-670D silicon diode cryogenic temperature sensor was also installed on the test plate to measure the cold end temperature. A Cryo-con Model 24C temperature controller was used to control the power of the heater. The warm heat exchanger (WHX) was exposed to the laboratory air and cooled by two heat sinks. A T-type thermocouple was used for measuring the surface temperature of the WHX. An Endevoc 8510B pressure senor was installed at the end of the transfer pipe connected to WHX. The other end of the transfer pipe was connected to the

pressure wave generator. The pressure profile measured by the pressure senor was used as the boundary condition in the forthcoming CFD models.

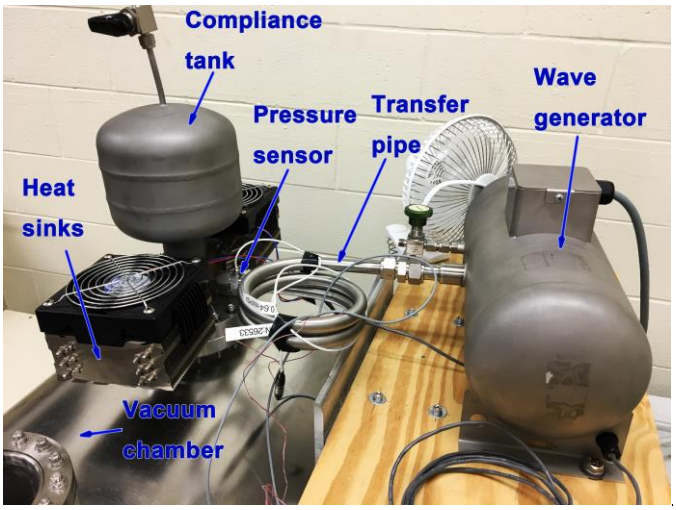

Figure 2. PTC prototype and vacuum chamber.

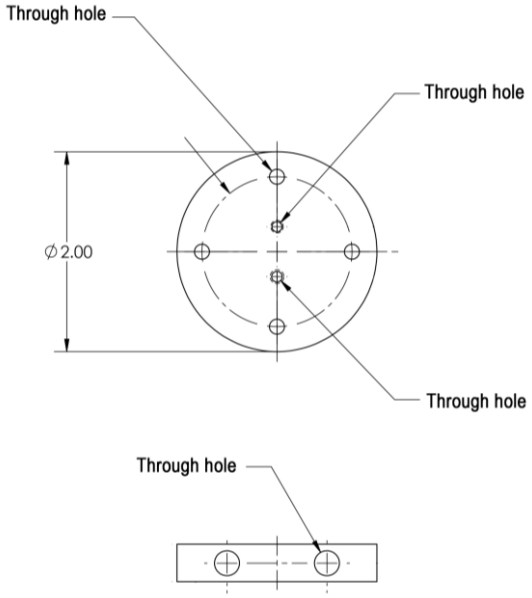

Figure 3. Drawing of the test plate that attached to the cold end.

3. CFD Methodology

In this section, the computational methodology is discussed including computational domain, boundary conditions and meshing. All CFD simulations were performed using the commercial package ANSYS FLUENT.

3.1. Computational domain and boundary conditions

The Stirling pulse tube cryocooler system in its entirety is normally too complex and computationally expensive for CFD simulation. Most interesting multi-dimensional features are located in the cold-tip assembly. Other components, e.g. inertance tube, compliance tank and transfer tube are 1D-like components. The conditions of the flow coming out from the inertance tube and transfer tube do not have a significant effect on the flow in the cold-tip assembly [9]. As a result, the sub-system representing the cold-tip assembly was taken as the computational domain in this work.

The computational domain is shown in figure 4. The geometry of the computational domain is very similar to the geometry of the experimentally tested PTC. A two-dimensional axis-symmetrical model was used to reduce the computational expense since the cold-tip was coaxial. As shown in figure 4, the regenerator, cold heat exchanger (CHX) and flow straighteners were treated as porous media in the model. All solid walls were omitted to reduce the overall computational expense. This is a reasonable approximation because in comparison with convection, the conduction heat transfer in the solid material is small [9]. Isothermal boundary conditions were used on the surfaces of the cold and warm ends of the cold-tip assembly. As shown in figure 4, the working temperature of the cooler varies from 313 K (warm end) to 77 K (cold end). The key performance indicator, the cycle-averaged cooling power, was calculated by averaging the instantaneous heat flux on the cold-end isothermal surface.

In the experiments, the cold-tip was connected to a transfer line and an inertance tube. The pressure wave generated by the pressure wave generator passes through the transfer line. The boundary condition in the conjunction between the transfer line and the cold-tip was modeled using the sinusoidal pressure profile measured in the experiments. The other boundary condition, at the junction between inertance tube and the cold-tip, was a sinusoidal mass flow rate. Direct measurement of the mass flow in inertance tube was impractical, however, and was therefore calculated by the one-dimensional tool, SAGE [12].

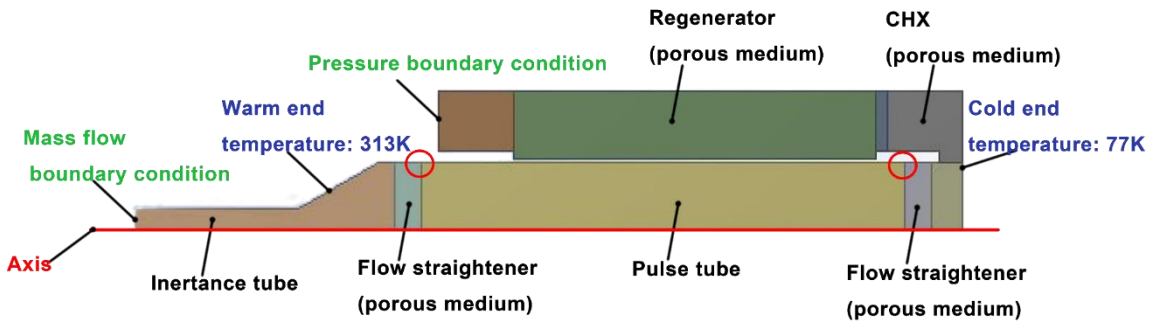

Figure 4. Computational domain and boundary conditions.

3.2. Meshing and modelling methodology

Figure 5 shows the mesh used in the simulations. Because the flow condition inside the pulse tube was conditionally turbulent according to Iguchi et al. [12], small and fine mesh was needed. The size of grid cells inside the pulse tube was equal to 1/127 of the diameter of the pulse tube. A minimum of 30 layers of inflation mesh was used on pulse tube wall. The height of the first cell layer was equivalent to about one wall unit, $\Delta y^+ \approx 1$, where $y^+ = y\frac{\sqrt{\tau_w/\rho}}{\nu}$ and τ_w is the wall shear stress. A coarser mesh was used for other regions, e.g., regenerator and CHX, where the flow details were not complex.

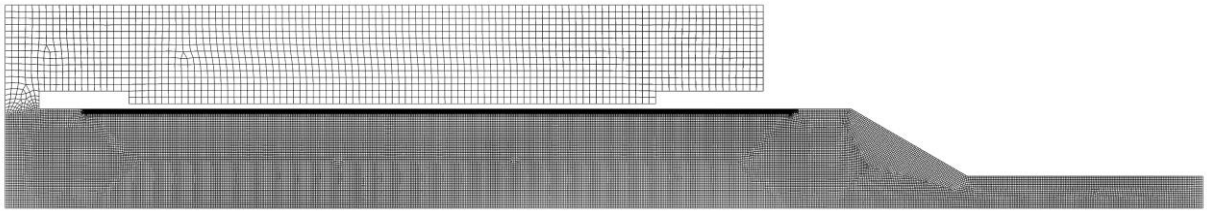

Figure 5. Mesh.

A laminar model and a time step equal to 1/400 of the period were used. Even though an implicit solver was used, the aforementioned time step yielded a value of peak courant number inside the pulse tube close to 1.

4. Results and discussion

4.1. Experiment

The cooling power of the PTC prototype has been measured at 400 W and 600 W driving powers, and 100 K and 77 K cold-end temperatures. These measurements were done at five inclination angles, including 0° (vertical position with cold head pointing downwards), 45°, 90°, 135° and 180° (vertical position with cold head pointing up).

The non-dimensional pulse tube convection number [7, 8], N_{ptc}, is normally used as an indicator of the gravitational sensitivity of PTC. It can be calculated as follow:

$$N_{PTC} = \frac{\omega^2 a^2}{g(\alpha_s D \sin\theta - L\cos\theta)}\sqrt{\left(\frac{\Delta T}{\Delta T_{avg}}\right)} \quad (1)$$

where ω is the angular frequency, a is the oscillation amplitude, g is gravitational acceleration, α_s is the fitting parameter, D is the pulse tube diameter, L is the pulse tube length, θ (larger than 90°) is the inclination angle from ideal vertical, ΔT is the temperature difference between the warm and cold ends, and T_{avg} is the average gas temperature in the pulse tube. Swift and Backhaus [7, 8] concluded that PTCs with small aspect ratios, D/L, have stable cooling performance when inclined if $N_{PTC} < 2$. When D/L is larger, the minimum safe value of N_{PTC} should be two times larger. However, Berryhill and Spoor

suggested that the safe factor (2) should be several times higher. By analyzing multiple experiments and simulations, Fang et al. [10] showed that an even higher safe factor is needed.

The N_{PTC} for the conditions tested in this work are shown in table 1. The oscillation amplitude cannot be measured experimentally. Therefore, it was calculated by CFD simulations. All of the cases should be stable if $N_{PTC} > 2$ was used as the safe factor.

Table 1. Non-dimensional pulse tube convection numbers of the pulse tube tested

Working condition		N_{ptc} at the inclination angle		
Driving power (W)	Cold-end temperature (K)	90°	135°	180°
600	100	60.6	26.1	26.6
400	100	28.4	12.3	12.5
600	77	18.3	7.9	8.1
400	77	13.9	6.0	6.1

Figure 6 presents the cooling performance of the inclined PTC in different working conditions. Figure 6a shows the cooling powers, and figure 6b shows the normalized cooling loses calculated from

$$L_\theta = \frac{cooling\ power\ at\ 0° - cooling\ power\ at\ \theta°}{cooling\ power\ at\ 0°} \quad (2)$$

Larger L_θ means the PTC loses more cooling power in comparison with the cooling in ideal vertical condition. In figure 6, notable cooling deteriorations can be observed when the PTC was inclined. At 135°, all cases had the lowest cooling power and therefore the worst performance. From figure 6b, when the PTC was driven by 400 W and the cold-end temperature was 77 K, the PTC lost all cooling power at 135°. With the same inclination angle, larger N_{PTC} implies that the performance is less sensitive to misalignment with gravity. The trend for the various driving powers and cold-end temperatures generally follow Swift and Backhaus's theory. However, the safe minimum value for N_{PTC} appears to be significantly higher than the value previously proposed by Swift and Backhaus.

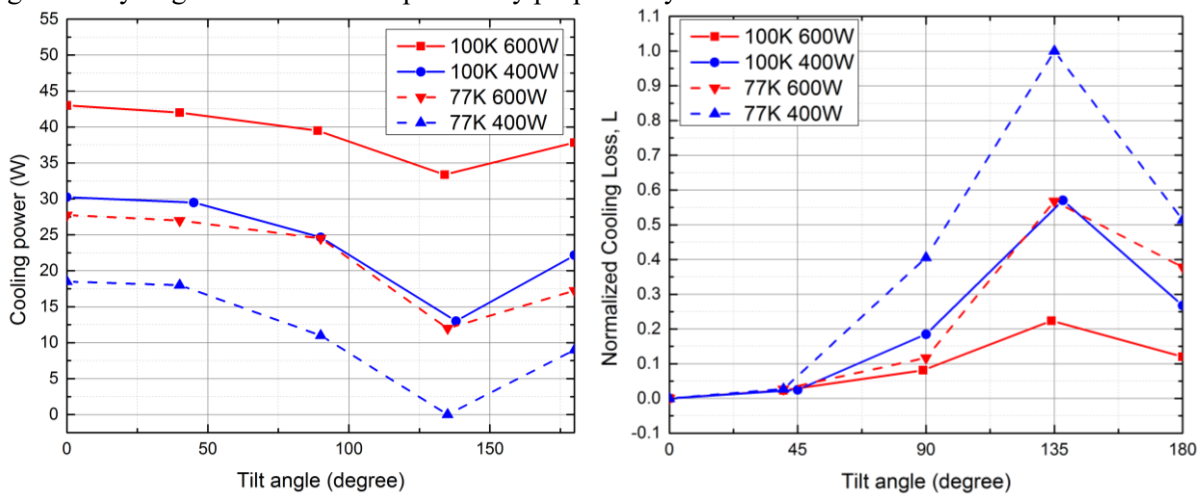

(a) Cooling power (b) Normalized cooling power

Figure 6. Cooling performances in different working conditions.

4.2. CFD Simulations

4.2.1. Perfect geometry, no minor geometric features and imperfection. As a starting point, a geometry with no minor off-design features and imperfections to result in streaming effects was simulated. Similar to the experiment, two driving powers (400 W and 600 W) and two cold-end temperatures (77 K and 100 K) were simulated. However, to accommodate axisymmetric modeling, only 0° and 180° inclination angle were simulated.

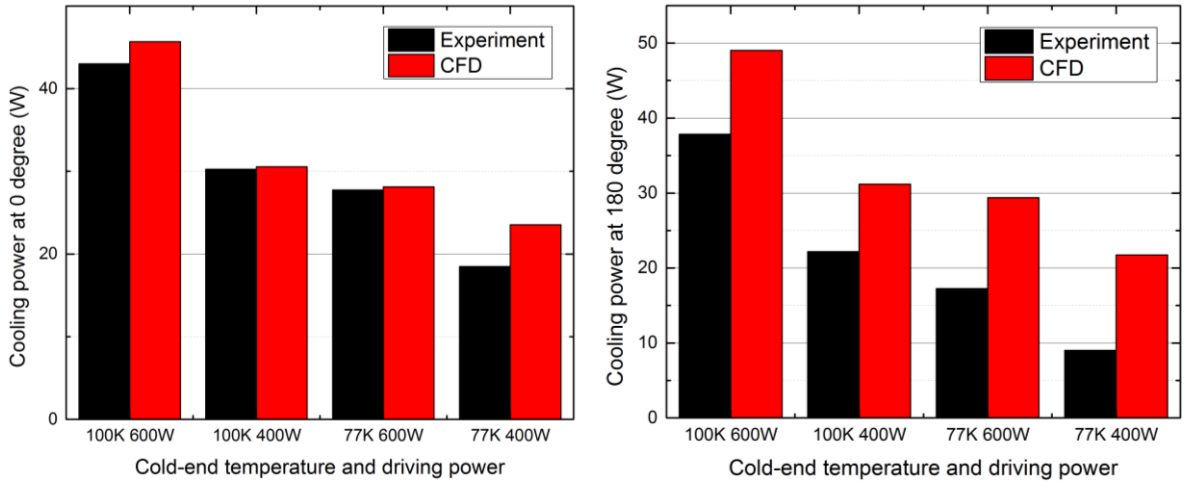

(a) vertical condition (b) upside point down condition

Figure 7. Comparison of the cooling power between experiment and CFD (no diameter mismatch).

The predicted cooling powers are shown in figure 7 along with the cooling power from experiment. As noted in figure 7a, the CFD simulations agree well with experiment for the case with 100 K cold-end temperature and 400 W driving power, and the case with 77 K cold-end temperature and 600 W driving power. For the other two cases, the differences between CFD and experiment are larger. It should be mentioned that one boundary condition was the mass flow rate calculated using SAGE [13] rather than experimental measurement. The SAGE predication could deviate from the real values. In figure 7b, the CFD simulation predicts almost no cooling deterioration when the cold-end is pointing up. Even though the CFD results did not agree with the experiment, it interestingly agrees with Swift and Backhaus's original safe condition which indicates that these cases should not be sensitive to misalignment with respect to gravity. The parametric study in the next section is meant to identify a potential cause of this discrepancy between CFD simulations and experiments.

4.2.2. Minor geometry features and imperfections. Some minor geometric features or imperfections may exist in a PTC, either by design or by manufacturing, that will normally not be resolved in CFD, e.g. tapered edges, small flow area changes, and small gaps in the junctions between components. Resolving these features can be computational expensive and unnecessary in most industrial applications. However, due to the special and complicated physics in a PTC, these small features/imperfections can be important. Therefore, a parametric study regarding minor geometry imperfection was carried out here.

The study focused on the most important junction (inside the red circle in figure 4), namely the junction between flow straightener chamber and pulse tube, indicated by Conrad et al. [11]. Figure 8 illustrates the parameters tested. The effective flow diameter of flow straightener is slightly larger than the diameter of the pulse tube, by the quantity a. Furthermore, b represents the size of a gap between flow straightener and the edge created by the diameter change. As shown in the right side of figure 8, two shapes of the edge, sharp edge and round edge ($r = a/2$), were studied. The PTC tested in Section 4.1 had similar geometric features shown in figure 8. However, the exact shape and dimensions were unknown because they were not carefully controlled during manufacturing. The geometry used in Section 4.2.1 was "perfect" and had $a = 0$ and thus $b = r = 0$.

The calculated cooling powers of various geometries are presented in table 2, where a, b and r are normalized with pulse tube diameter, D. Even though the dimension of the geometric features are very small, the cooling performance results show their significant effects. In general, rounding or tapering the edge helped improve the cooling performance. The size of the gap did not make a notable difference. However, having a gap resulted to a huge drop (around 80%) in the cooling power. The effect of minor geometric features is more significant when the cooler is upside down. Even though the data points are limited at this point in the study, they underscore the detrimental effect of off-design geometric features, in particular when a number of such off-design features are concurrently present.

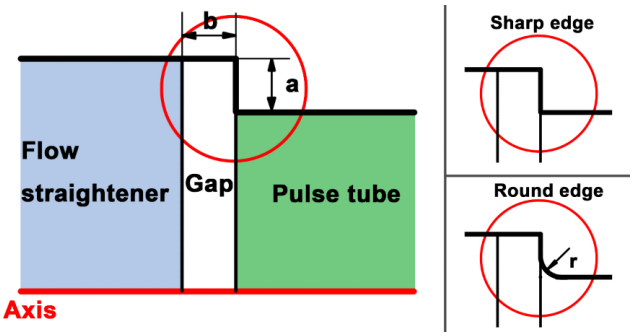

Figure 8. Parameters of the geometric features in the conjunction between flow straightener and pulse tube; right side figures indicate the shape of the edge.

Table 2. CFD calculated cooling power for geometries having different diameter change (*a*), gap size (*b*), edge shape (*r*) and inclination angle.

a/D	*b/D*	*r/D*	Cooling power (W)	
			At 0°	At 180°
1/80	0	0	-	1.88
1/160	0	0	22.60	3.58
1/160	0	1/320	29.54	25.97
1/160	1/640	1/320	-	4.29
1/160	1/320	1/320	-	4.78
1/160	1/160	1/320	19.05	7.50

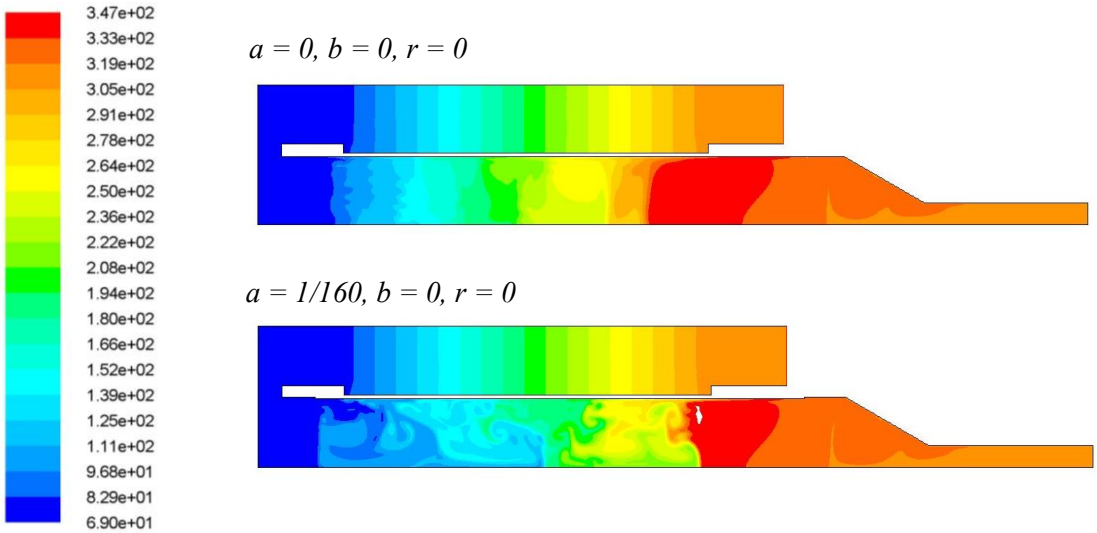

Figure 9. Comparison of the temperature distributions between perfect geometry (upper figure) and imperfect geometry (lower figure) at 180°.

Figure 9 shows the temperature contours of two geometries at 180°. The upper figure has perfect geometry, while the lower figure has a diameter mismatch in the junction between the pulse tube and flow straightener. It can be inferred that this minor geometric feature caused significant chaos and mixing in the pulse tube.

5. Conclusion

In this work, a PTC prototype was experimentally tested to investigate the effect of misalignment with respect to gravity on the performance of pulse tube cryocoolers. The cooling performance of the PTC for varying driving powers, cold-end temperatures and inclination angles was analyzed. When inclined, notable cooling deteriorations were noticed in the experiments. In terms of general trends, the sensitivity

of the tested PTC with respect to misalignment with gravity generally agreed with the trend predicted by Swift and Backhaus's theory [7, 8] if the criterion for the safe operation was several times larger. A sub-system CFD study having very similar but perfect geometry as the PTC prototype was also carried out. The calculated performance, for the ideal vertical configuration with cold tip at the bottom, agreed with the experiment. The predicted performance of the PTC for conditions where the PTC was tilted with respect to gravity deviated from experimental measurements. However, the CFD predicted cooling deterioration agreed with Swift and Backhaus's original theory. A careful review of the results shown that the difference between experimentally measured and CFD-calculated performance parameters can be due to the combined effect of some seemingly minor off-design geometric features or imperfections not resolved in CFD. One specific feature, namely a diameter mismatch at the junction between a flow straightener and pulse tube, was identified and was parametrically studied. The results indicated that the cooling performance of the PTC was sensitive to this and other seemingly minor geometric features. The current 2D CFD model was not able to fully resolve the asymmetric minor geometric features in the experiment. As a result, the results from the CFD simulation did not exactly match the experimental results. Further study of these sensitivities is underway.

6. References

[1] D. L. Gardner and G. W. Swift, "Use of inertance in orifice pulse tube refrigerators," *Cryogenics,* vol. 37, no. 2, pp. 117-121, 1997.

[2] S. W. Zhu, S. L. Zhou, N. Yoshimura and Y. Matsubara, "Phase shift effect of the long neck tube for the pulse tube refrigerator," in *Cryocoolers 9*, Springer US, 1997, pp. 269-278.

[3] J. R. Olson and G. W. Swift, "Acoustic streaming in pulse tube refrigerators: tapered pulse tubes," *Cryogenics,* vol. 37, no. 12, pp. 769-776, 1997.

[4] D. Gedoen, "DC gas flows in Stirling and pulse tube cryocoolers," in *Cryocooler 9*, vol. 9, Springer US, 1997, pp. 385-392.

[5] R. P. Taylor, "Development and Experimental Validation of a Pulse-Tube Design Tool Using Computational Fluid Dynamics," 2009.

[6] G. Thummes, M. Schreiber, R. Landgraf and C. Heiden, "Convective heat losses in pulse tube coolers: effect of pulse tube inclination," in *Cryocooler 9*, Springer US, 1997, pp. 393-402.

[7] G. Swift and S. Backhaus, "Why high-frequency pulse tubes can be tipped," in *Cryocoolers 16*, Spring US, 2008.

[8] G. W. Swift and S. Backhaus, "The pulse tube and the pendulum," *The Journal of the Acoustical Society of America,* vol. 126, no. 5, pp. 2273-2284, 2009.

[9] T. I. Mulcahey, "Convective Instability of Oscillatory Flow in Pulse Tube Cryocoolers due to Asymmetric Gravitational Body Force," Phd Thesis, Georgia Institute of Technology, 2014.

[10] T. Fang, T. I. Mulcahey, R. P. Taylor, P. S. Spoor, T. J. Conrad and S. M. Ghiaasiaan, "Method for Estimating Off-Axis Pulse Tube Losses," *Cryogenics,* 2017.

[11] T. Conrad, M. G. Pathak, S. M. Ghiaasiaan and C. Kirkconnell, "The effect of component junction tapering on miniature cryocooler performance," *AIP Conference Proceedings,* vol. 1434, no. 1, pp. 435-442, 2012.

[12] M. IGUCHI, M. OHMI and K. MAEGAWA, "Analysis of free oscillating flow in a U-shaped tube," *Bulletin of JSME,* vol. 25, no. 207, pp. 1398-1405, 1982.

[13] D. Gedeon, Sage User's Guide v11 Edition, 16922 South Canaan Rd.: Gedeon Associates, 2016.